Phase Diagram of Hydrogen and a Hydrogen-Helium Mixture at Planetary Conditions by Quantum Monte Carlo Simulations

Guglielmo Mazzola,[1,*] Ravit Helled,[2] and Sandro Sorella[3]
[1]*Theoretische Physik, ETH Zurich, 8093 Zurich, Switzerland*
[2]*Institute for Computational Science, Center for Theoretical Astrophysics and Cosmology, University of Zurich, 8057 Zurich, Switzerland*
[3]*International School for Advanced Studies (SISSA) and INFM Democritos National Simulation Center, via Bonomea 265, 34136 Trieste, Italy*

(Received 2 November 2017; published 12 January 2018)

Understanding planetary interiors is directly linked to our ability of simulating exotic quantum mechanical systems such as hydrogen (H) and hydrogen-helium (H-He) mixtures at high pressures and temperatures. Equation of state (EOS) tables based on density functional theory are commonly used by planetary scientists, although this method allows only for a qualitative description of the phase diagram. Here we report quantum Monte Carlo (QMC) molecular dynamics simulations of pure H and H-He mixture. We calculate the first QMC EOS at 6000 K for a H-He mixture of a protosolar composition, and show the crucial influence of He on the H metallization pressure. Our results can be used to calibrate other EOS calculations and are very timely given the accurate determination of Jupiter's gravitational field from the NASA Juno mission and the effort to determine its structure.

DOI: 10.1103/PhysRevLett.120.025701

For a few decades the link between the uncertainty of the hydrogen equation of state (EOS) and the internal structure of Jupiter (and other gaseous planets) has been investigated and many efforts to model Jupiter's interior have been carried out [1–4]. The computation of an EOS from first principles requires solving a many-body quantum mechanical problem, a task which is beyond the currently available theoretical and computational capabilities. In practice, we must resort to several approximations. The first is to decouple the ionic and electronic problems and consider the ions as classical or quantum particles, determining their motion by following the Born-Oppenheimer potential energy surface. The second approximation concerns the description of the electronic interaction, and in particular the exchange interaction, due to the Pauli exclusion principle.

The standard approach to EOS calculations relies on density functional theory (DFT), which targets the tridimensional electronic density rather than the (N_e electrons) many-body wave function. Its success and simplicity have led to a widespread application in materials science and to the development of several software packages that allow fast and reproducible calculations [5]. Although DFT is *formally* exact, the explicit functional form to describe the exchange and correlation (XC) effects between electrons remains approximated [6]. Indeed, a systematic and efficient route to improve the XC functional is still lacking. Therefore, in practical solid-state calculations, benchmarks against experimental data are often required to validate the XC functional used to describe the system in a satisfactory manner.

Hydrogen-rich compounds under pressure, both in the low temperature solid and in the liquid phase, remain a challenge to DFT simulations due to the interplay of strong correlation and noncovalent interactions between the atoms. DFT calculations with different functionals can produce different results, with the expected metallization pressure varying over a range of 100 to 200 GPa (Fig. 1) [7,8] for pure H.

This uncertainty affects the EOS calculation, and therefore, also planetary modeling. Currently, planetary modelers use hydrogen EOSs that have been derived from DFT data [18,19], using a specific choice for the density functional, the Perder-Burke-Erzenhof (PBE) functional [20]. It has been demonstrated that a change in the functional, for example, using one which includes an empirical van der Waals dispersion interaction (vdW-DF2 [21]), results in a different EOS. In this case the calculated pressure at a given density is larger by ∼10%–20% [8] compared to PBE. On the other hand, given the accurate determination of Jupiter's gravitational field by the Juno mission, it was shown that the EOSs should be known with accuracy of ∼1% in order to constrain Jupiter's internal structure [22].

In the case of hydrogen at high pressure, it is difficult to assess *a posteriori* the quality of the DFT approximation, benchmarking with experiments, for various reasons. The first is that experiments typically have uncertainties larger than 1% for both Hugoniot [22,23] and phase boundary measurements. In this second case, experiments performed with different compression techniques do not always agree. For example, static compression with laser heating [16,17,24] and dynamic compression measurements (with deuterium) [15] differ by ∼150 GPa at 1500 K for what concerns the location of the first-order liquid-liquid transition (LLT) between the molecular and the atomic fluids.

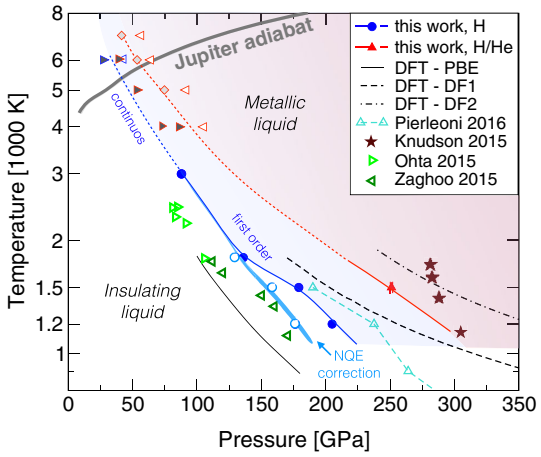

FIG. 1. Phase diagram of dense hydrogen (H) and a hydrogen-helium (H-He) mixture. We show the liquid-liquid transition (LLT) between the insulating-molecular and the metallic-atomic fluid (shaded area). Theoretical results have been obtained under the classical nuclei approximation unless otherwise indicated. Solid symbols refer to our QMC LLT for pure H (blue circles) and for the H-He mixture (red triangle). Solid blue and red lines indicate a first-order LLT. At high temperatures, the empty (solid) left (right) triangles correspond to simulations displaying a clear atomic (molecular) behavior, while red diamonds represent an intermediate behavior (see Supplemental Material [9]). These points are used to constrain the phase boundaries where the transition is continuous (dashed blue and red lines). Also shown is Jupiter's adiabat (gray line) as calculated by Miguel *et al.* [3]. Pure H first-order LLT predictions by QMC simulations [from Pierleoni *et al.* [14] (cyan)] and by DFT using different XC functionals, PBE, vdW-DF1, and DF2 (taken from Knudson *et al.* [15]), are also shown. Other symbols refer to metallization experimental data. Shown are experiments with static compression [16,17] (light green and dark green triangles) and deuterium shockwave [15] (brown stars).

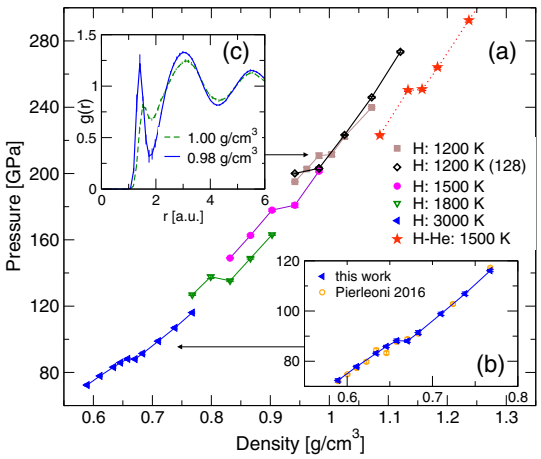

FIG. 2. Equations of state across first-order transitions. Pressure versus density for pure H and four temperatures (1200, 1500, 1800, and 3000 K, 64 particles) and for a H-He mixture (at 1500 K, 128 particles). For H at 1200 K, we present results also for a 128 particles system (black diamonds). The transition pressure obtained with the 128 particle setup is smaller by 8 (2) GPa compared to the 64 particle case. The first-order transition is identified by a *plateau* in the EOS. The discontinuity is more evident at lower temperatures but is still visible at 3000 K (a). Panel (b) shows the EOS computed by Pierleoni *et al.* [14]. Panel (c) shows two proton radial pair distributions for pure H at 1200 K, for the two densities close to the LLT. The sudden disappearance of the molecular peak is consistent with a first-order transition.

On the simulation side, the PBE functional [25–28] seems to agree qualitatively with the experimental Refs. [17,24], whereas vdW-DF2 [8] is more compatible with Refs. [15,29]. Therefore, the possibility of validating existing EOSs, and reconcile simulations with experiments, is highly desirable. This is also true in the case of the H-He mixture, where experiments are still missing.

Recently, quantum Monte Carlo (QMC) approaches emerged as competitive tools to accurately solve electronic problems [30] thanks to the new generations of supercomputers. Since QMC simulation is a wave-function-based method (unlike DFT), the scheme to obtain consistently better results is simple and relies on the variational principle. Indeed, the accuracy of the calculations improves as the richness of the many-body electronic wave function increases. In our variational approach, a systematic way to improve the wave function is by enlarging the localized atomic basis set that defines our quantum state. The unprecedented availability of computational resources led to the development of QMC algorithms that combine efficiently the simulations of electrons with ion dynamics [31–33]. Unlike the DFT method, which is well established and widely used, the QMC technique is still relatively new and is used by a smaller community of developers with various implementations and algorithms that are difficult to benchmark. However, the few QMC results for the H phase diagram, until now, have not agreed well. In particular, while all QMC simulations agreed qualitatively on a larger dissociation and metallization pressure for pure dense liquid H, compared to PBE, the precise location was not well determined due to different QMC implementations, variational wave function, and finite-size effects errors [14,28,33–35].

We perform simulations with 64 and 128 H atoms for the H compound and with 118 H and 10 He atoms for the H-He mixture (see Supplemental Material for details [9]). For the mixture we use $x = n_{\mathrm{He}}/n_{\mathrm{H}} \approx 0.08475$, which is smaller than the protosolar value of 0.0969 [36] and slightly larger than Jupiter's value of 0.0785(18) [37]. We first trace the liquid-liquid transition for pure H at intermediate temperatures, between 1200 and 1800 K, using a 64 hydrogen atom system. The first-order transition is characterized by a discontinuity in the EOS (see Fig. 2) and in the proton-proton radial pair distribution function $g(r)$ [Fig. 2(c)]. It is found to occur at densities of ~0.8–1 $\mathrm{g\,cm^{-3}}$ and pressures of ~200 GPa at 1200 K,

~180 GPa at 1500 K, and ~135 GPa at 1800 K. The LLT seems to involve mostly a local rearrangement of the liquid structure [see Fig. 2(c) and also Fig. S1 in Supplemental Material [9]) and lies between the two recent experiments obtained using static compression by Silvera and coworkers [17,24] and the dynamic compression measurements (with deuterium) by Knudson *et al.* [15], although it is much closer to Refs. [17,24]. Moreover, the systematic errors caused by the finite size (cf. the 64 and 128 particle data series in Fig. 2) and basis set (cf. Fig. S2 in Supplemental Material [9]) can shift the LLT by ~10 GPa; therefore, our results are compatible with the recent QMC prediction by Pierleoni *et al.* [14]. However, in order to better compare our results with these low temperature experiments, the quantum nature of the protons (here assumed as classical particles) also needs to be considered. Indeed, when we correct our results with these nuclear quantum effects (NQE), the agreement with static compression experiments improves significantly [17,24,38] (see Fig. 1). In this work we do not directly perform simulations beyond the classical nuclei approximation, using path-integral-based methods as in Ref. [14], where electronic QMC simulations with or without NQE are reported. They show that NQE shifts the LLT to smaller pressures at most by 35 GPa at 1200 K and by 25 GPa at 1500 K. Here we simply apply these shifts to our LLT to derive the phase boundary in Fig. 1 and compare to experiments [17]. Note that PBE underestimates the metallization pressure compared to QMC simulations (Fig. 1), and the disagreement with experiments further increases if NQEs are taken into account.

In this work, we correct the systematic errors that affected our previous results and led to a much larger metallization pressure: the electronic size effects errors, not adequately removed in Refs. [33,34] and a localized basis set [39] that was too small (1Z) to describe the metal and the insulator with the same accuracy [35]. In addition, our previous studies used a less efficient optimization method; indeed, the so-called "linear method" [40] requires a careful generalization to the case of complex wave functions (see Supplemental Material for details [9]). Nevertheless, as discussed above, our predicted LLT is now affected by an uncertainty of ~10 GPa. We believe that computing the H phase diagram with an accuracy of 1 GPa is still beyond the present numerical capabilities, especially at low temperatures.

After benchmarking our technique for pure H, we next investigate a H-He mixture at 1500 K. We find that He, even in a small fraction $x \approx 0.085$, changes qualitatively the physics of the system. In particular, its presence stabilizes the hydrogen molecules (H_2), delaying the onset of metallization towards higher densities. This effect is also observed in DFT-PBE simulations (cf. Vorberger *et al.* [41]). However, our direct QMC simulations clearly identify the molecular dissociation in the H-He mixture at ~250 GPa with 1500 K, and a density ~1.1 g cm^{-3} [see Fig. 2(a)], resulting in a shift of ≈70 GPa compared to the pure H system.

An important open question concerns the location of the H critical point, which is the end point of the first-order LLT. Above the critical point, in the P-T phase diagram the dissociation occurs smoothly. While recent EOS calculations suggest that Jupiter's adiabat lies above the critical point, implying the lack of first-order phase transition, its possible occurrence has a direct consequence on the internal structure of gas giant planets. If the phase transition is of first order, it would suggest a density discontinuity within the planet's interior, and the possibility of a non-adiabatic interior as well as for discontinues in the heavy elements distribution.

Also in this case a clear experimental consensus is still missing. McWilliams *et al.* [29] do not find evidence for a first-order transition below 150 GPa, while Ohta *et al.* [16] suggest instead the persistence of a first-order LLT well above 2000 K. Motivated by these studies, we perform additional simulations at higher temperatures. In the pure H case we are able to resolve a small discontinuity in the EOS and the $g(r)$ at 3000 K (see Fig. 2). Although a finer mesh of densities is required, as well as an extended finite-size scaling in order to precisely resolve the existence of the *plateau* in the EOS, the observed feature suggests the existence of a critical point above the previously expected temperature of 1500–2000 K [26,28] (with the notable exception of Norman and Saitov [42] who predict a critical temperature of 4000 K from PBE simulations).

Finally, we calculate QMC and DFT-PBE EOSs at 6000 K over a wide range of densities, spanning a pressure range between 30 (40) and 260 (300) GPa for pure H (H-He mixture). This isotherm is expected to cross Jupiter's adiabat around 60 GPa, i.e., at 0.6 Mbar.

We find that QMC simulation, at a given density, predicts a pressure which is ~5% smaller than PBE; i.e., at a fixed pressure QMC simulation predicts a denser liquid compared to PBE (see Fig. 3). Our QMC EOS for pure H is compatible with available QMC data at 6000 K from Refs. [43,44]. This difference with PBE becomes larger at small pressures (~10%), across the continuous phase transition. Also shown in the figure is a comparison of our calculation with the two popular H EOSs for planetary interiors; the H-REOS.3 [19] and MH-SCvH-H [18], both of which are based on PBE simulations. We show that H-REOS.3 is in perfect agreement with our DFT calculations, whereas the MH-SCvH-H EOS (extrapolating the data in the limiting case of pure H [3]) is closer to our QMC calculation. The disagreement between the two EOSs could be caused by the extrapolation [3], and it seems that the disagreement between these two groups is linked to the calculated entropies [3,45]. Either way, it is clear that QMC simulation implies a denser EOS for H at Jupiter's conditions, which translates to an envelope that is poor in heavy elements. If this is indeed the case, it introduces new challenges in understanding Jupiter's current structure and origin [3,45,46]. Since Jupiter structure models with a

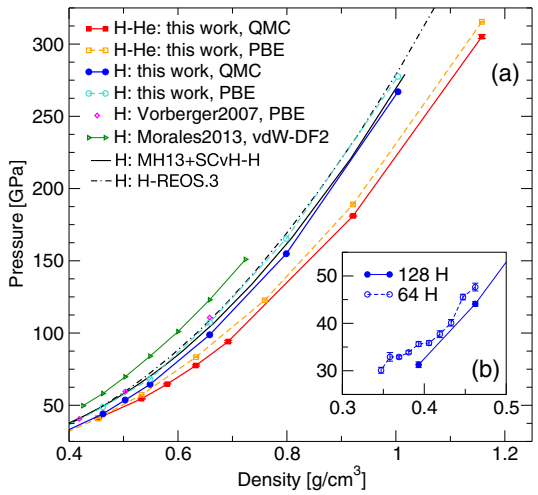

FIG. 3. Equations of state at 6000 K. Panel (a) shows the EOS with QMC simulations (solid lines) and DFT PBE (dashed) for pure H (circles) and the H-He mixture (triangles) inferred using a supercell of 128 particles. For the pure H case we also report PBE calculations of Vorberger *et al.* [41], simulations with the vdW-DF2 functional [8], and the commonly used EOSs for pure H, H-REOS.3 [19] (dot-dashed black line) and MH-SCvH-H [18] (continuous black line). In the inset (b) we show additional simulations, using a 64 hydrogen system and a finer density mesh, to investigate the nature of the pure H dissociation. Given the moderate slope and the statistical error bars (≈0.5 GPa) of the EOS, resolving any discontinuity is not possible at this stage.

denser EOS for H lead to a very low atmospheric metallicity, with Z being 0.01 or even smaller, using QMC EOS is expected to reduce the metallicity even further. However, it should be noted that these estimates have been performed for a fully adiabatic Jupiter, and a nonadiabatic Jupiter can be more metal rich [47,48]. In addition, in order to accurately estimate the effect of the QMC EOS on Jupiter's structure, a much larger parameter space of temperatures and pressures should be simulated.

Regarding the nature of the phase transition at 6000 K, we find that for H our QMC simulation indicates that a continuous transition is most likely to occur, as a clear EOS discontinuity is absent (see inset of Fig. 3). This means that the critical temperature for pure H is between 3000 and 6000 K. We can further constrain the location of the LLT by performing simulations at different temperatures and densities, identifying the largest (smallest) pressure at which a clear molecular peak persists (disappear).

For pure H, the continuous molecular dissociation occurs mainly between 31 and 44 GPa at 6000 K. This value is in very good agreement with the recent x-ray scattering measurements of a continuous metallization transition at around 50 GPa and 5000 K [49] (cf. Fig. 1). For the H-He mixture, we directly perform simulations at temperatures between 4000 and 7000 K (see Supplemental Material Figs. S3 and S4 [9]), relevant for planetary interiors (Fig. 1). At 6000 K, H_2 dissociation in the H-He mixture

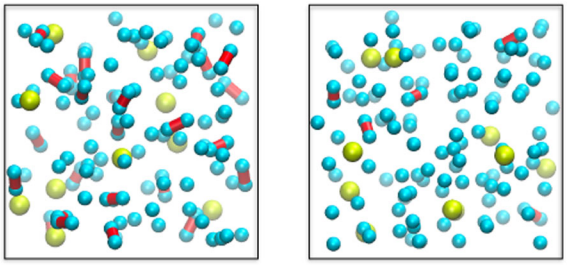

FIG. 4. Snapshots of a H-He mixture simulation. Shown are two typical snapshots of our MD simulations. The cyan, yellow, and red colors represent the 108 H atoms, 10 He atoms, and H molecule bonds (H_2), respectively. For sake of visualization, a H_2 molecule is defined when two hydrogen atoms are closer than 1.6 bohr. These two structures (projected on the x-y plane), the first (second) represents a mainly molecular (atomic) phase, are computed at different iterations of the same MD simulation, at a temperature of 6000 K and density of ∼0.53 g/cm^3 [$P = 54.3(3)$ GPa], i.e., near the LLT.

occurs mainly between 42 and 64 GPa. Moreover, at a density of ∼0.53 g cm^{-3} and P ≈ 54 GPa, we observe the stability of a mixed phase as the simulation quickly fluctuates between a pure atomic and a mainly molecular liquid (see Fig. 4). Therefore, our calculations show that the continuous transition from molecular to metallic hydrogen in Jupiter's conditions occurs at ∼0.4–0.6 Mbar. This provides further constraints for Jupiter structure models, as the transition pressure between the two envelopes cannot be used as a free parameter [3,50]. A transition pressure of that value implies a larger mass of heavy elements in Jupiter's deep interior [3].

Our *ab initio* simulations for a hydrogen-helium mixture, the first obtained with QMC simulation, open a new opportunity to better constrain the behavior of H and H-He in planetary conditions. We show that even a small concentration of He of ≈8.5% has an important impact on the metallization pressure of the liquid, as the dissociation is delayed by 70 GPa at low temperature (1500 K) and by a maximum of 30 GPa at 6000 K.

QMC techniques do not only allow for an explicit description of electron correlations, and therefore are systematically improvable, but they also have the potential to expand and become commonly used with the future generations of massively parallel supercomputers. Several new research directions can be envisaged, from the calculation of a new QMC-based EOS for pure H, to the simulations of heavier elements at planetary conditions.

A new generation of QMC calculations could tackle even larger systems (comparable with DFT simulations) and address further questions relevant for planetary interiors such as the precise location of the critical point in the H-He phase diagram, the miscibility of He and other heavier materials in H, and other intriguing physical and chemical transformations such as methane and ammonia dissociation at high pressures.

We acknowledge discussions with N. Nettelmann, C. Pierleoni, and B. Militzer. G. M. was supported by the European Research Council through ERC Advanced Grant SIMCOFE and the Swiss National Science Foundation (SNSF) through the National Competence Centers in Research MARVEL. R. H. acknowledges support from the Swiss National Science Foundation (SNSF) Grant No. 200021_169054. Computational resources were provided by CINECA in Bologna, AICS-Riken project n.hp170079, and by the Swiss National Supercomputing Centre CSCS.

*gmazzola@phys.ethz.ch

[1] T. Guillot, The interiors of giant planets: Models and outstanding questions, Annu. Rev. Earth Planet Sci. **33**, 493 (2005).

[2] N. Nettelmann, A. Becker, B. Holst, and R. Redmer, Jupiter models with improved *ab initio* hydrogen equation of state (H-REOS.2), Astrophys. J. **750**, 52 (2012).

[3] Y. Miguel, T. Guillot, and L. Fayon, Jupiter internal structure: The effect of different equations of state, Astron. Astrophys. **596**, A114 (2016).

[4] B. Militzer, F. Soubiran, S. M. Wahl, and W. Hubbard, Understanding Jupiter's interior, J. Geophys. Res. Planets **121**, 1552 (2016).

[5] K. Lejaeghere *et al.*, Reproducibility in density functional theory calculations of solids, Science **351**, aad3000 (2016).

[6] K. Burke, Perspective on density functional theory, J. Chem. Phys. **136**, 150901 (2012).

[7] S. Azadi and W. M. C. Foulkes, Fate of density functional theory in the study of high-pressure solid hydrogen, Phys. Rev. B **88**, 014115 (2013).

[8] M. A. Morales, J. M. McMahon, C. Pierleoni, and D. M. Ceperley, Nuclear Quantum Effects and Nonlocal Exchange-Correlation Functionals Applied to Liquid Hydrogen at High Pressure, Phys. Rev. Lett. **110**, 065702 (2013).

[9] See Supplemental Material at http://link.aps.org/supplemental/10.1103/PhysRevLett.120.025701 which contains additional details of the methods, extended simulation results, and additional Refs. [10–13].

[10] M. Motta *et al.*, Towards the Solution of the Many-Electron Problem in Real Materials: Equation of State of the Hydrogen Chain with State-of-the-Art Many-Body Methods, Phys. Rev. X **7**, 031059 (2017).

[11] M. Dagrada, S. Karakuzu, V. L. Vildosola, M. Casula, and S. Sorella, Exact special twist method for quantum Monte Carlo simulations, Phys. Rev. B **94**, 245108 (2016).

[12] T. H. Dunning, Gaussian basis sets for use in correlated molecular calculations. I. The atoms boron through neon and hydrogen, J. Chem. Phys. **90**, 1007 (1989).

[13] P. Giannozzi *et al.*, QUANTUM ESPRESSO: A modular and open-source software project for quantum simulations of materials, J. Phys. Condens. Matter **21**, 395502 (2009); http://www.QUANTUM-ESPRESSO.org.

[14] C. Pierleoni, M. A. Morales, G. Rillo, M. Holzmann, and D. M. Ceperley, Liquid-liquid phase transition in hydrogen by coupled electron-ion Monte Carlo simulations, Proc. Natl. Acad. Sci. U.S.A. **113**, 4953 (2016).

[15] M. D. Knudson, M. P. Desjarlais, A. Becker, R. W. Lemke, K. R. Cochrane, M. E. Savage, D. E. Bliss, T. R. Mattsson, and R. Redmer, Direct observation of an abrupt insulator-to-metal transition in dense liquid deuterium, Science **348**, 1455 (2015).

[16] K. Ohta, K. Ichimaru, M. Einaga, S. Kawaguchi, K. Shimizu, T. Matsuoka, N. Hirao, and Y. Ohishi, Phase boundary of hot dense fluid hydrogen, Sci. Rep. **5**, 16560 (2015).

[17] M. Zaghoo, A. Salamat, and I. F. Silvera, Evidence of a first-order phase transition to metallic hydrogen, Phys. Rev. B **93**, 155128 (2016).

[18] B. Militzer and W. B. Hubbard, *Ab initio* equation of state for hydrogen-helium mixtures with recalibration of the giant-planet mass-radius relation, Astrophys. J. **774**, 148 (2013).

[19] A. Becker, W. Lorenzen, J. J. Fortney, N. Nettelmann, M. Schöttler, and R. Redmer, *Ab initio* equations of state for hydrogen (H-REOS.3) and helium (He-REOS.3) and their implications for the interior of brown dwarfs, Astrophys. J. Suppl. Ser. **215**, 21 (2014).

[20] J. P. Perdew, K. Burke, and M. Ernzerhof, Generalized Gradient Approximation Made Simple, Phys. Rev. Lett. **77**, 3865 (1996).

[21] K. Lee, E. D. Murray, L. Kong, B. I. Lundqvist, and D. C. Langreth, Higher-accuracy van der Waals density functional, Phys. Rev. B **82**, 081101 (2010).

[22] J. M. McMahon, M. A. Morales, C. Pierleoni, and D. M. Ceperley, The properties of hydrogen and helium under extreme conditions, Rev. Mod. Phys. **84**, 1607 (2012).

[23] W. J. Nellis, Dynamic compression of materials: Metallization of fluid hydrogen at high pressures, Rep. Prog. Phys. **69**, 1479 (2006).

[24] V. Dzyabura, M. Zaghoo, and I. F. Silvera, Evidence of a liquid-liquid phase transition in hot dense hydrogen, Proc. Natl. Acad. Sci. U.S.A. **110**, 8040 (2013).

[25] S. Scandolo, Liquid-liquid phase transition in compressed hydrogen from first-principles simulations, Proc. Natl. Acad. Sci. U.S.A. **100**, 3051 (2003).

[26] W. Lorenzen, B. Holst, and R. Redmer, First-order liquid-liquid phase transition in dense hydrogen, Phys. Rev. B **82**, 195107 (2010).

[27] I. Tamblyn and S. A. Bonev, Structure and Phase Boundaries of Compressed Liquid Hydrogen, Phys. Rev. Lett. **104**, 065702 (2010).

[28] M. A. Morales, C. Pierleoni, E. Schwegler, and D. M. Ceperley, Evidence for a first-order liquid-liquid transition in high-pressure hydrogen from *ab initio* simulations, Proc. Natl. Acad. Sci. U.S.A. **107**, 12799 (2010).

[29] R. S. McWilliams, D. A. Dalton, M. F. Mahmood, and A. F. Goncharov, Optical Properties of Fluid Hydrogen at the Transition to a Conducting State, Phys. Rev. Lett. **116**, 255501 (2016).

[30] W. Foulkes, L. Mitas, R. Needs, and G. Rajagopal, Quantum Monte Carlo simulations of solids, Rev. Mod. Phys. **73**, 33 (2001).

[31] C. Attaccalite and S. Sorella, Stable Liquid Hydrogen at High Pressure by a Novel *Ab Initio* Molecular-Dynamics Calculation, Phys. Rev. Lett. **100**, 114501 (2008).

[32] C. Pierleoni, D. M. Ceperley, and M. Holzmann, Coupled Electron-Ion Monte Carlo Calculations of Dense Metallic Hydrogen, Phys. Rev. Lett. **93**, 146402 (2004).
[33] G. Mazzola, S. Yunoki, and S. Sorella, Unexpectedly high pressure for molecular dissociation in liquid hydrogen by electronic simulation, Nat. Commun. **5**, 3487 (2014).
[34] G. Mazzola and S. Sorella, Distinct Metallization and Atomization Transitions in Dense Liquid Hydrogen, Phys. Rev. Lett. **114**, 105701 (2015).
[35] G. Mazzola and S. Sorella, Accelerating *Ab Initio* Molecular Dynamics and Probing the Weak Dispersive Forces in Dense Liquid Hydrogen, Phys. Rev. Lett. **118**, 015703 (2017).
[36] J. N. Bahcall, M. H. Pinsonneault, and G. J. Wasserburg, Solar models with helium and heavy-element diffusion, Rev. Mod. Phys. **67**, 781 (1995).
[37] U. von Zahn, D. M. Hunten, and G. Lehmacher, Helium in Jupiter's atmosphere: Results from the Galileo probe helium interferometer experiment, J. Geophys. Res. Planets **103**, 22815 (1998).
[38] V. E. Fortov *et al.*, Phase Transition in a Strongly Nonideal Deuterium Plasma Generated by Quasi-Isentropical Compression at Megabar Pressures, Phys. Rev. Lett. **99**, 185001 (2007).
[39] S. Sorella, N. Devaux, M. Dagrada, G. Mazzola, and M. Casula, Geminal embedding scheme for optimal atomic basis set construction in correlated calculations, J. Chem. Phys. **143**, 244112 (2015).
[40] C. J. Umrigar, J. Toulouse, C. Filippi, S. Sorella, and R. G. Hennig, Alleviation of the Fermion-Sign Problem by Optimization of Many-Body Wave Functions, Phys. Rev. Lett. **98**, 110201 (2007).
[41] J. Vorberger, I. Tamblyn, B. Militzer, and S. A. Bonev, Hydrogen-helium mixtures in the interiors of giant planets, Phys. Rev. B **75**, 024206 (2007).
[42] G. Norman and I. Saitov, Critical point and mechanism of the fluid-fluid phase transition in warm dense hydrogen, Dokl. Phys. **62**, 294 (2017).
[43] M. A. Morales, C. Pierleoni, and D. M. Ceperley, Equation of state of metallic hydrogen from coupled electron-ion Monte Carlo simulations, Phys. Rev. E **81**, 021202 (2010).
[44] N. M. Tubman, E. Liberatore, C. Pierleoni, M. Holzmann, and D. M. Ceperley, Molecular-Atomic Transition along the Deuterium Hugoniot Curve with Coupled Electron-Ion Monte Carlo Simulations, Phys. Rev. Lett. **115**, 045301 (2015).
[45] W. B. Hubbard and B. Militzer, A preliminary Jupiter model, Astrophys. J. **820**, 80 (2016).
[46] S. M. Wahl *et al.*, Comparing Jupiter interior structure models to Juno gravity measurements and the role of a dilute core, Geophys. Res. Lett. **44**, 4649 (2017).
[47] J. Leconte and G. Chabrier, A new vision of giant planet interiors: Impact of double diffusive convection, Astron. Astrophys. **540**, A20 (2012).
[48] A. Vazan, R. Helled, M. Podolak, and A. Kovetz, The evolution and internal structure of Jupiter and Saturn with compositional gradients, Astrophys. J. **829**, 118 (2016).
[49] P. Davis *et al.*, X-ray scattering measurements of dissociation-induced metallization of dynamically compressed deuterium, Nat. Commun. **7**, 11189 (2016).
[50] R. Helled and T. Guillot, Interior models of Saturn: Including the uncertainties in shape and rotation, Astrophys. J. **767**, 113 (2013).